Biochemistry

 Volume 30, Number 2 January 15, 1991

Accelerated Publications

Packing Characteristics of Highly Unsaturated Bilayer Lipids: Raman Spectroscopic Studies of Multilamellar Phosphatidylcholine Dispersions

Burton J. Litman,[‡,§] E. Neil Lewis,[‖] and Ira W. Levin*[,‖]

Department of Biochemistry, University of Virginia Health Sciences Center, Charlottesville, Virginia 22908, and Laboratory of Chemical Physics, National Institute of Diabetes and Digestive and Kidney Diseases, National Institutes of Health, Bethesda, Maryland 20892

Received October 19, 1990; Revised Manuscript Received November 14, 1990

ABSTRACT: The thermotropic properties and acyl chain packing characteristics of multilamellar dispersions of highly unsaturated lipids were examined by Raman spectroscopy. Bilayer assemblies were composed of POPC (1-palmitoyl-2-oleoylphosphatidylcholine), PAPC (1-palmitoyl-2-arachidonylphosphatidylcholine), and PDPC (1-palmitoyl-2-docosahexaenoylphosphatidylcholine), lipid systems possessing saturated *sn*-1 chains and unsaturated *sn*-2 chains with one, four, and six double bonds, respectively. Raman spectra were recorded in the acyl chain 2800–3100-cm^{-1} carbon–hydrogen (C–H) stretching and 1100–1200-cm^{-1} carbon–carbon (C–C) stretching mode regions, spectral intervals reflecting both the inter- and intrachain order/disorder properties of the various lipid dispersions. In order to obtain C–H stretching mode spectra relevant solely to the *sn*-1 chains of PAPC and PDPC, liquid-phase spectra of arachidonic and docosahexaenoic acid, respectively, were subtracted from the observed phospholipid spectra. The unsaturated *sn*-2 chains of PAPC and PDPC undergo minimal conformational reorganizations as the bilayers pass from the gel to liquid-crystalline phases. Phase transition temperatures, T_m, derived from statistically fitting the temperature-dependent Raman spectral data are approximately −2.5, −22.5, and −3 °C for POPC, PAPC, and PDPC, respectively. As the degree of unsaturation increases from POPC to PAPC and PDPC, the cooperativity of the phase transition, as measured by its breadth, decreases. Estimates of the transition widths from the temperature profiles are approximately 15 °C for PAPC and 20 °C for PDPC. The behavior of various Raman spectral parameters for the lipid gel phase reflects the formation of lateral microdomains, or clusters, whose packing properties maximize the van der Waals interactions between *sn*-1 chains. Since studies have shown that the conformational equilibrium of an integral membrane protein can be modulated by varying either the lipid *sn*-2 chain unsaturation or the bilayer temperature (Mitchell et al., 1990), the microdomain heterogeneity characteristic, for example, of highly unsaturated lipid bilayers may provide a mechanism for controlling the physical properties necessary for optimizing membrane functions associated with the structural reorganizations of integral proteins.

Biological membranes are heterogeneous lipid assemblies composed of mixtures of molecular species varying in headgroup and hydrocarbon chain composition. Phospholipids, with saturated and unsaturated acyl chains in the *sn*-1 and *sn*-2 glycerol backbone positions, respectively, represent the most abundant membrane lipid class (White, 1973). Although virtually all naturally occurring lipids contain multiply unsaturated *sn*-2 chains, physical studies have largely focused on systems comprised of either symmetric saturated chains or those with *sn*-2 chains containing only a single double bond (Levin, 1984; Thompson & Huang, 1986). The importance, however, of polyunsaturation in modulating membrane bilayer properties has been clearly demonstrated by animal studies in which dietary fatty acid composition was carefully controlled. In particular, for a wide variety of cellular membranes isolated from several tissue sources, the proportions of saturated to unsaturated lipids, as well as the degree of bilayer hydro-

* Author to whom correspondence should be addressed.
‡ University of Virginia Health Sciences Center.
§ Partially supported by NIH Grant EY00548.
‖ National Institutes of Health.

carbon unsaturation, remained relatively constant to external lipid supplementation (Murchie, 1988). The significance of acyl chain unsaturation is also emphasized by specific systems, such as the retinal rod outer segment disk membrane, in which nearly 50% of the total *sn*-2 acyl chains are derived from docosahexaenoic acid, a 22-carbon chain containing six double bonds (Nielson et al., 1970; Miljanich et al., 1979).

Although the lipid bilayer acts primarily to maintain the cell's permeability barrier and to serve as a matrix for various bilayer constituents, integral membrane proteins are responsible for most of the active processes carried out by biological membranes. Membrane functions are to a large degree mediated by conformational changes which result in the activation of integral membrane proteins, as, for example, the opening of either a membrane channel or a receptor binding site. These structural reorganizations are often associated with a positive volume change of the protein in which the energy required for a rearrangement in the plane of the membrane will in part be determined by the packing properties of the lipid bilayer. Since biological membranes exist in an essentially isothermal state, the modulation of the physical properties of the bilayer necessary to maintain a functional mileu for integral proteins must be achieved by regulating the fatty acid composition of the lipid matrix. Therefore, information concerning the bilayer packing and dynamics of phospholipid molecules with chains of varying amounts of *sn*-2 unsaturation becomes critical in elucidating mechanisms by which compositional changes in membrane bilayer lipids modify the conformational and hence the functional characteristics of integral membrane proteins.

Among the limited physical studies performed on phospholipid bilayers containing polyunsaturated acyl chains, differential scanning calorimetry illustrates the unusual bilayer characteristics of these assemblies. For example, the gel to liquid-crystalline phase transition temperatures, T_m, for a series of phosphatidylcholines with a saturated 20:0 carbon *sn*-1 chain and an *sn*-2 chain varying in double bond composition from 20:0 to 20:4 showed a discontinuity in the decrease in T_m with increasing degree of unsaturation (Keough et al., 1987). In other studies fluorescence depolarization measurements carried out on POPC,[1] PAPC, and PDPC exhibited a progressive increase, with increasing degree of unsaturation, of a parameter reflecting the packing free volume within the hydrophobic region of the bilayer (Straume & Litman, 1987).

In this study we shall examine by vibrational Raman spectroscopy the thermotropic properties of model phosphatidylcholine bilayer assemblies whose variation in hydrocarbon unsaturation reflects the naturally occurring *sn*-2 acyl chains in biological membranes. In general, vibrational data derived from Raman spectroscopy offer a direct and noninvasive method of obtaining structural, packing, and dynamic properties of membrane systems [see, for example, Levin (1984)]. Since molecular details pertaining to polyunsaturated phospholipids are exceedingly sparse, we compare specifically in this study the phase transition behavior and acyl chain packing characteristics, as a function of temperature, of multilamellar assemblies of POPC, PAPC, and PDPC, containing respectively one, four, and six double bonds in the *sn*-2 chain position. The two vibrational spectral intervals discussed for these systems, namely, the lipid acyl chain 2900-cm^{-1} C–H and 1100-cm^{-1} C–C stretching mode regions, reflect both the inter- and intrachain order/disorder properties of the various lipid dispersions.

Experimental Procedures

Samples of POPC, PAPC, and PDPC were purchased from Avanti Polar Lipids Inc. and used without further purification. Fatty acid samples of arachidonic and docosahexaenoic acid were obtained from Sigma Chemical Co. Chloroform stock solutions of each lipid were evaporated under a stream of nitrogen and further dired on a vacuum line for 24 h to ensure total solvent removal. BHT at about a 500:1 molar ratio was immediately added to both PAPC and PDPC prior to drying to protect these lipids against peroxidation. Multilamellar model membrane suspensions were formed by vortexing dry lipids in either H_2O or D_2O buffer solutions at about 20–30% concentration on a weight/volume basis. POPC and PAPC were suspended in H_2O, while PDPC was suspended in D_2O. The suspensions contained 50 mM NaCl and 50 μM DTPA. Lipid peroxidation was inhibited by the presence of DTPA and by sealing the samples under nitrogen in Kimex glass capillary tubes. POPC and PAPC were spun in a desk-top centrifuge for 10–15 min prior to collection of spectra; the PDPC sample was spun in a Beckman Tl-100 centrifuge at 89000*g* for 20 min at 5 °C. Samples were allowed to equilibrate in the sample holder at least 45 min prior to data collection.

Raman spectra were recorded on a Spex Ramalog 6 dispersive spectrometer equipped with holographic gratings and interfaced to an LSI-11-based laboratory data acquisition system controlled by software developed in this laboratory. A Coherent Innova Model 100 argon ion laser provided 250 mW of 514.5-nm laser excitation at the sample. Spectra were recorded in both the C–H and C–C stretching mode regions for the lipids and in the C–H stretching mode region for the acids. Typically, for each data set 3–10 scans were averaged at an instrumental resolution of approximately 5 cm^{-1} and at a scan rate of 1 cm^{-1} s^{-1}. After collection, the data files were transferred via our laboratory network to a Sun UNIX workstation for processing. The temperature profiles presented for POPC, PAPC, and PDPC in Figure 3, as well as the T_m's and phase transition breadths derived for these lipids, represent data collected from two, four, and one separate heating curves, respectively.

Spectra used in the construction of the temperature profiles for all three lipid dispersions were recorded at approximately 1 °C temperature increments throughout the phase transition region. Spectra were recorded in an ascending temperature mode, 3-min equilibration time being allowed between data points. Temperature control was achieved by enclosing the samples in a thermoelectrically regulated cell assembly under computer control. With this configuration sample temperatures may be maintained reliably to within ±0.1 °C.

Results and Discussion

Raman spectra were collected in the methylene chain 2900-cm^{-1} C–H stretching mode region for aqueous dispersions of multilamellar vesicles of POPC, PAPC, and PDPC, while spectra of PDPC were also collected in the acyl chain 1100-cm^{-1} C–C stretching mode region. The spectrum for PDPC in the C–H stretching mode interval displays features reflecting both the saturated *sn*-1 and unsaturated *sn*-2 acyl chains (Figure 1, dashed line). Although this is a highly complex, congested spectral contour, the vibrational transitions of the phospholipid molecules contributing to the Raman intensity in this spectral region are well understood (Snyder et al., 1978; Synder & Scherer, 1979; Snyder & Strauss, 1982). Several

[1] Abbreviations: POPC, 1-palmitoyl-2-oleoylphosphatidylcholine (*sn*-2 chain unsaturated at Δ9); PAPC, 1-palmitoyl-2-arachidonoylphosphatidylcholine (*sn*-2 chain unsaturated at Δ5,8,11,14); PDPC, 1-palmitoyl-2-docosahexaenoylphosphatidylcholine (*sn*-2 chain unsaturated at Δ4,7,10,13,16,19); DTPA, diethylenetriaminepentaacetic acid; BHT, butylated hydroxytoluene.

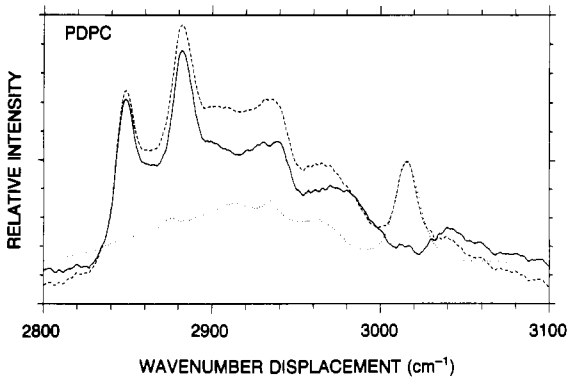

FIGURE 1: Raman spectra of PDPC multilayers in the gel state at −20.5 °C (dashed line) and docosahaxaenoic acid in the liquid state at 6.2 °C (dotted line). The solid line shows the spectrum of PDPC after subtraction of the liquid-phase docosahaxaenoic acid spectrum and represents the saturated chain contribution to the overall spectral contour.

important spectral features are clearly discernible. Peaks centered at approximately 2850 and 2880 cm^{-1} are assigned to the saturated *sn*-1 chain methylene symmetric and asymmetric stretching modes, respectively. The feature observed at approximately 2935 cm^{-1} is assigned to a superposition of a Fermi resonance component of the acyl chain terminal methyl symmetric stretching mode and Fermi components of the methylene asymmetric stretching modes, while the peak at about 3015 cm^{-1} reflects the olefinic C–H stretching modes of the unsaturated *sn*-2 chain. Thus, in principle, this spectral region allows one to monitor independently the bilayer behavior of both the *sn*-1 and *sn*-2 acyl chains.

Raman spectroscopic studies of phospholipid bilayers (Kouaouci et al., 1985; Vincent & Levin, 1988; Yeager & Gaber, 1987) have focused primarily on lipids with saturated acyl chains. Such studies have firmly established and defined Raman spectroscopic markers which are highly sensitive to lipid bilayer packing and gel to liquid-crystalline phase transition properties (Huang et al., 1982; Mushayakarara et al., 1982; Lewis et al., 1986). For example, the C–H stretching mode peak height intensity ratios for the methylene symmetric and asymmetric stretching modes (I_{2850}/I_{2880}) provide information on predominantly lipid interchain packing behavior, while the intensity ratios for the complex Fermi resonance feature at 2935 cm^{-1} and the methylene asymmetric stretching modes (I_{2935}/I_{2880}) contain information reflecting both the inter- and intrachain order/disorder characteristics. In the C–C stretching mode region the peak height intensity ratios of the ~1090- and ~1130-cm^{-1} transitions, assigned to gauche and trans chain conformers, respectively, provide direct measures of intrachain disorder.

Since the C–H stretching mode region spectroscopic markers described above relate for the most part to coupled methylene oscillator systems (Snyder et al., 1978; Snyder & Schachtschneider, 1963), the intensity arising from the interrupted methylene groups in the unsaturated chain must be subtracted in order to effectively derive *sn*-1 chain properties. Thus, we consider the C–H stretching mode region, to a first approximation, a linear combination of spectra originating from the coupled oscillator saturated *sn*-1 chain and the unsaturated *sn*-2 chain, which does not exhibit the unique spectral properties of extended segments of coupled methylene moieties. Appropriate subtraction of the *sn*-2 chain spectral contributions, therefore, affords a means of monitoring the effect of *sn*-2 unsaturation on the packing properties of the saturated *sn*-1 chains and, in turn, allows the inter- and intramolecular packing properties of the overall more complex bilayer to be studied with the previously defined and well-understood peak height intensity ratios.

In order to obtain spectra reflecting solely the *sn*-1 saturated chains of PAPC and PDPC, liquid-phase spectra of arachidonic and docosahexaenoic acid, respectively, were subtracted from the observed phospholipid spectra. Before spectral subtraction, the acid spectra were appropriately scaled to the intensity of the ~3015-cm^{-1} olefinic C–H stretching modes observed in the lipid dispersions. While the solid- and liquid-phase spectra of the acids are quite similar, the vibrational frequencies and line widths for the olefinic C–H stretching modes of the *liquid* acids most closely matched the analogous parameters of the various lipid spectra. Therefore, only liquid-phase acid spectra were used in the subtraction process for both the gel and liquid-crystalline phases of the given phospholipid. (Polarization effects originating from the use of a liquid-phase acid sample are essentially removed by not preferentially selecting a polarization when spectra are being recorded. The scattered radiation representing all polarizations is passed through a scrambler prior to entering the monochromator.) Figure 1 shows the observed Raman spectrum of PDPC at −20 °C in the C–H stretching mode region before and after subtraction (dashed and solid line, respectively) of the normalized liquid-phase spectrum of docosahexaenoic acid (dotted line). No spectral subtraction was required for the 1100-cm^{-1} C–C stretching mode region, since docosahexaenoic acid, which mimics the *sn*-2 unsaturated lipid chain of PDPC, has little or no intensity in this spectral interval. Thus, the 1100-cm^{-1} region reflects directly the coupled oscillator properties of the saturated *sn*-1 chain. No analogous acid subtraction was performed for the C–H stretching mode region of POPC, since the *sn*-2 chain of this lipid, which contains only one double bond at the 9,10 chain position, yields spectra closely resembling those of fully saturated chains; that is, the C–H stretching mode region of POPC monitors the average order/disorder characteristics of both chains.

Analysis of the temperature dependence of the subtracted spectra both above and below the gel to liquid-crystalline phase transition, which are analogous to Raman spectra previously obtained for diacyl saturated systems (Huang et al., 1982; Levin, 1984), indicates that the major contributions to the intensity changes observed in the C–H stretching mode region of PAPC and PDPC are associated primarily with the melting of the saturated *sn*-1 chain. In contrast, the general frequency and line-width insensitivities to wide ranges in temperature, including melting, of the spectral data for the arachidonic and docosahexaenoic acids suggest that the conformational freedom of the lipid unsaturated *sn*-2 chain represented by these moieties is relatively restricted in comparison to that of the saturated *sn*-1 chain. That is, we expect the *sn*-2 chains of PAPC and PDPC to undergo little conformational reorganizations as the lipid bilayers pass from the gel to the liquid-crystalline phase.

Figure 2 presents Raman spectra in the acyl chain C–H stretching mode regions for POPC, PAPC, and PDPC (panels A–C, respectively) in both the gel and liquid-crystalline phases. The spectra shown for PAPC and PDPC are those obtained after the spectral subtraction, allowing for the elimination of the *sn*-2 chain components. These data demonstrate the concerted spectral changes that occur specifically for saturated chain lipid dispersions as they pass from the relatively ordered low-temperature gel phase to a more disordered liquid-crystalline phase (Levin, 1984). As stated previously, probes for intermolecular and intramolecular order/disorder phenomena are reflected in the relative intensities of the 2850, 2880, and

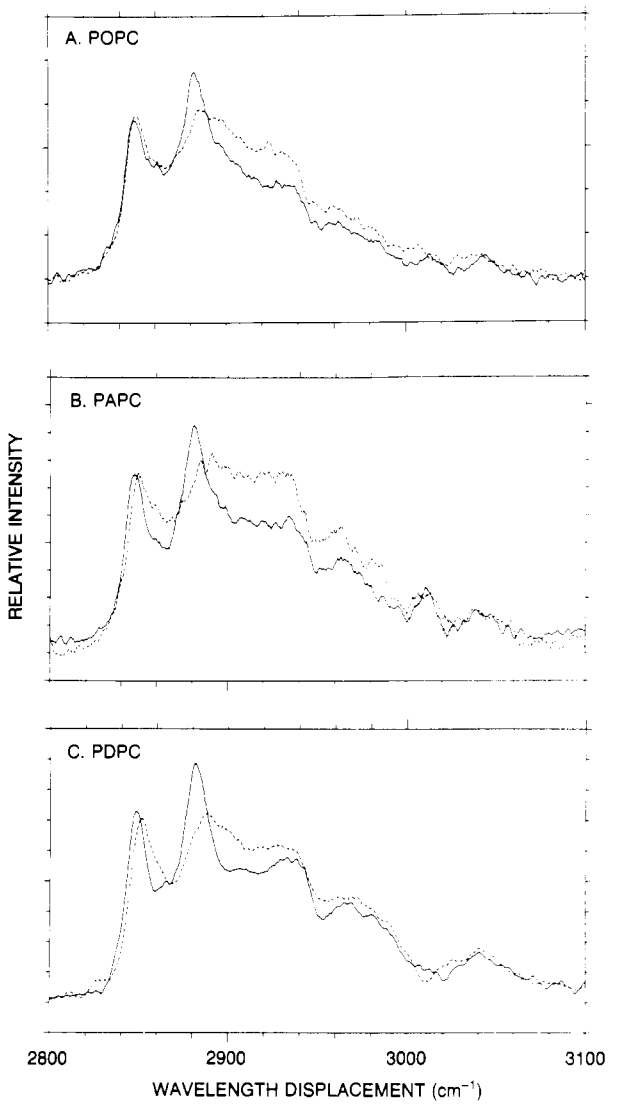

FIGURE 2: Raman spectra of all three lipid dispersions in the C–H stretching mode region both above and below the gel to liquid-crystalline phase transition. (A) POPC, (solid line, −16 °C; dashed line, 14.9 °C); (B) PAPC (solid line, −36 °C; dashed line, 40 °C); (C) PDPC (solid line, −20.5 °C; dashed line, 17 °C).

2935-cm^{-1} modes. The spectra show that the derived peak height intensity ratios, measuring primarily intermolecular order (I_{2850}/I_{2880}), increase for all three lipid dispersions from approximately 0.75 to 1.0 as they pass from their gel to liquid-crystalline phases, while the I_{2935}/I_{2880} parameter, measuring intramolecular reorganizations superimposed on intermolecular effects, exhibits changes from approximately 0.5 to 0.9. The temperature profiles derived from the two intensity ratios are summarized in Figure 3 for all three lipid dispersions. This figure reflects relatively cooperative phase transition behavior for the three systems when the I_{2935}/I_{2880} peak height intensity profiles are primarily being monitored (panels A–C); these phase transition characteristics are not discerned as readily by the I_{2850}/I_{2880} intensity ratios (panels D–F). As the degree of unsaturation increases from POPC to PAPC and PDPC, the cooperativity of the phase transition, as monitored by its breadth, decreases. Estimates of the transition widths from the temperature profiles in panels A–C in Figure 3 yield approximately 6 °C for POPC, while for PAPC and PDPC the transition widths increase to about 15 and 20 °C, respectively. The gel to liquid-crystalline phase transition temperatures, T_m, derived from the temperature profiles fit to the data, are approximately −2.5 °C for POPC, −22.5 °C for PAPC, and −3 °C for PDPC. Therefore, the T_m values for these lipids do not vary monotonically with the introduction of increased chain length and unsaturation. It is of interest to note that although these phase transitions are readily monitored by Raman spectroscopy, the phase transition for PDPC could not be observed by scanning calorimetry (unpublished observations).

The I_{2850}/I_{2880} temperature profiles in Figure 3 for PAPC and PDPC, panels E and F, respectively, display broad melting curves with a significant scatter in the data in contrast to the more familiar sigmoidal curves displayed for saturated chain bilayers. Since the sample chamber is thermostatted and sample temperatures are carefully regulated and monitored, the scatter of points, representing sequential equilibrium sample temperatures in the profiles, is considered to be characteristic of PAPC and PDPC multilayers. In as much as the I_{2850}/I_{2880} intensity ratio monitors bilayer chain–chain interactions, the observations suggest that the introduction of high unsaturation into the *sn*-2 chain leads to marked changes, or fluctuations, in the packing arrangements of the hydrocarbon chains as the temperature of the bilayer increases. In contrast, the reduced scatter of the I_{2935}/I_{2880} temperature contours relative to the I_{2850}/I_{2880} profiles, where the former intensity ratio is also sensitive to the formation of gauche conformers along the chain, indicates that a lesser perturbation is introduced into the intrachain bilayer order/disorder term with increasing unsaturation. We emphasize, however, that for the I_{2935}/I_{2880} intensity parameter the absolute phase transition cooperativity, which is related to chain melting or increased trans/gauche isomerization, decreases for the various lipid dispersions with increasing unsaturation. The increase in T_m reflected by the I_{2935}/I_{2880} profiles for PDPC relative to PAPC is consistent with the observed decrease in fluctuations of the PDPC bilayer order/disorder indices as a function of temperature. That is, a relatively more stable bilayer matrix would be associated with the less chaotic change in melting parameters. The observed differences between these intensity ratio probes may be directly compared to POPC or studies on diacyl saturated chain lipid dispersions (Huang et al., 1982; Yeager & Gaber, 1987; Lavaille & Levin, 1980), where both the I_{2935}/I_{2880} and I_{2850}/I_{2880} intensity ratios show narrower, well-defined sigmoidal phase transition curves.

Figure 4 displays the Raman spectral data obtained for PDPC in the acyl chain 1100-cm^{-1} C–C stretching mode region. This figure generally indicates a more cooperative phase transition with significantly less scatter between consecutive data points than that obtained from the I_{2935}/I_{2880} parameters for PDPC. (The data for each spectral region are taken sequentially while the sample remains equilibrated at a given temperature.) The I_{1090}/I_{1130} intensity ratio, which specifically measures intrachain order/disorder processes, provides further evidence that the predominant effect of unsaturation is preferentially manifested in changes in the intermolecular interactions of the extended bilayer structure. That is, the profile monitoring intrachain trans/gauche isomerization shows well-behaved characteristics, while the parameters measuring interchain order/disorder processes demonstrate chaotic behavior. It is interesting to note that the I_{2935}/I_{2880} ratio, which has both interchain and intrachain components, shows an intermediate level of both overall phase transition cooperativity and chaotic behavior between sequential temperatures.

In the highly unsaturated PAPC and PDPC systems, the nature of the melting of the *sn*-1 chain, coupled with the important observation that the 2800–3100-cm^{-1} spectral contours resemble ensembles of saturated hydrocarbon chains

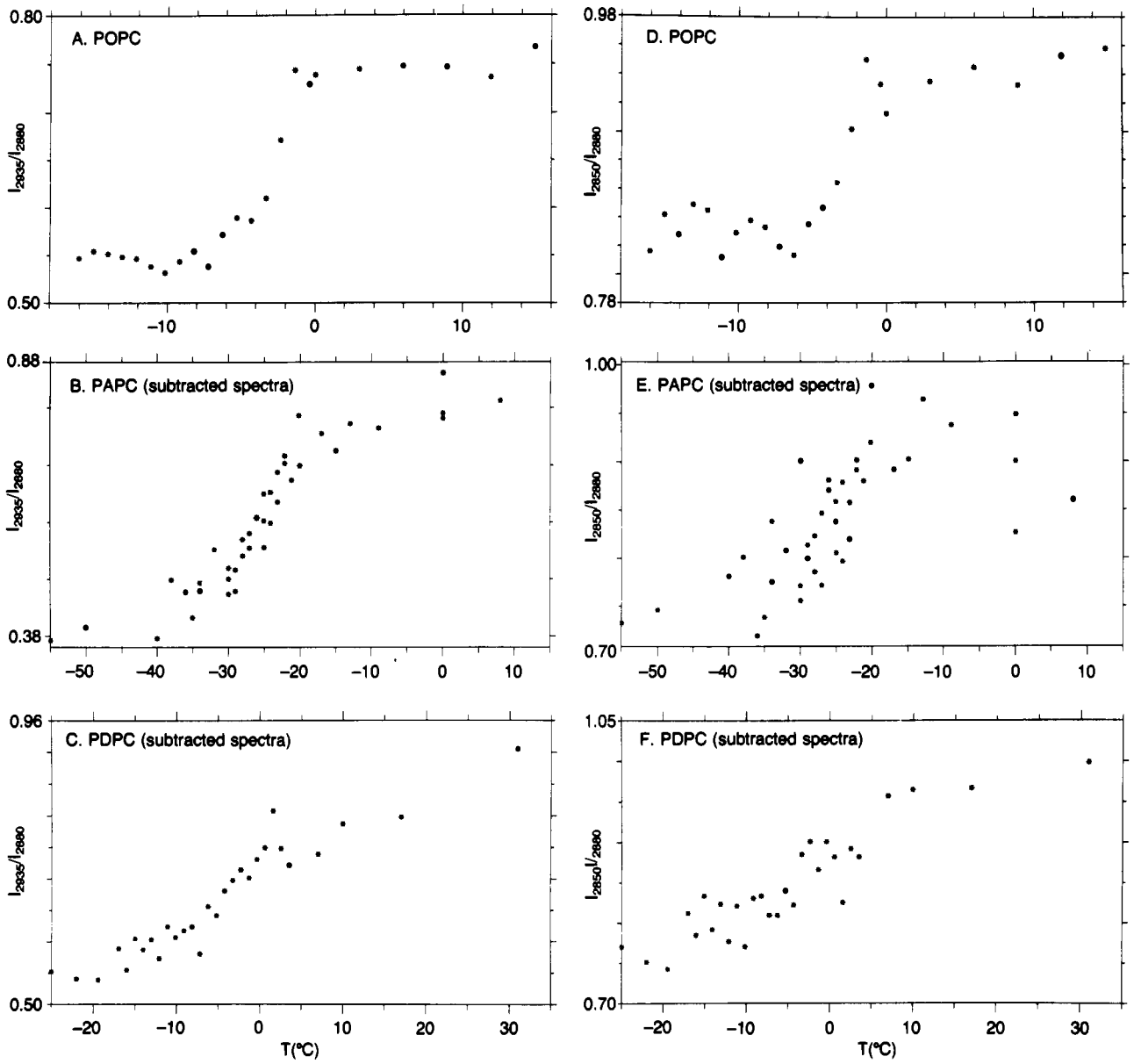

FIGURE 3: Summary of the temperature profiles derived from the C–H stretching mode region for POPC, PAPC, and PDPC. Panels A–C plot the peak height intensity ratios I_{2935}/I_{2880} against temperature, while panels D–F present the I_{2850}/I_{2880} intensity ratios versus temperature. The ratios used for PAPC and PDPC are those calculated after subtraction of the appropriate acid spectrum. The figure shows relative order, phase transition temperatures, phase transition cooperativity, and microheterogeneity for the three lipid dispersions.

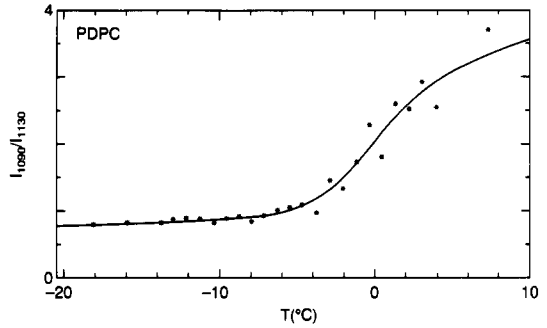

FIGURE 4: Summary of the C–C stretching mode region temperature profile for PDPC. The figure plots the I_{1090}/I_{1130} intensity ratio versus temperature and shows increasing intrachain disorder with increasing temperature.

similar to that of saturated diacyl liposomes in contrast to isolated acyl chains (Mendelsohn & Koch, 1980; Gaber & Petticolas, 1977; Snyder et al., 1978), leads to the conclusion that in the bilayer PAPC and PDPC molecules pack in a manner promoting the interaction of their respective *sn*-1 chains. The relative scatter of the I_{2850}/I_{2880} intensity ratio profiles below and throughout a somewhat ill-defined phase transition region strongly suggests a melting of gel-phase clusters. In contrast to POPC and particularly to saturated lipid systems, the melting curves of PAPC and PDPC multilayers generally reflect a high degree of microheterogeneity in their packing characteristics below and within their phase transition regions. Profiles constructed from the temperature dependence of the methylene symmetric stretching mode *frequencies*, which is a probe devoid of any potential artifacts introduced into the data by spectral subtraction (data not shown), show similar microdomain melting behavior.

Our results indicate that the saturated *sn*-1 chains of PAPC and PDPC assemble into gel-phase lattice arrangements which undergo gel to liquid-crystalline phase transitions similar to the broadened transition behavior observed for perturbed saturated diacyl chain phosphatidylcholine multilayers. The highly unsaturated *sn*-2 acyl chains, however, display a reduced conformational flexibility, as demonstrated by the spectral

insensitivity of the unsaturated acids in the C–H stretching mode regions to large changes in temperature. This is further illustrated by the fact that for these lipid dispersions the frequency of the peak centered at approximately 3015 cm^{-1}, corresponding to the olefinic C–H stretching mode, decreases during melting of POPC but remains unchanged in PAPC and PDPC. This behavior is consistent with a lack of flexibility for the multiply unsaturated *sn*-2 chains. Thus, the *sn*-2 chains for PAPC and PDPC contribute little to changes in the spectral characteristics derived for the saturated *sn*-1 chains during the lipid-phase transition. In addition, the reduced cooperativity of the phase transitions, as determined by the breadths of the temperature profiles, indicates the presence of microdomains or cluster formation in the PAPC and PDPC bilayers. Since the *sn*-1 chain peak height intensity ratios, derived after subtraction of the appropriate acid spectrum to compensate for the *sn*-2 chain contributions, reflect ensembles of saturated chains undergoing gel to liquid-crystalline phase transitions, we conclude that the PAPC and PDPC molecules pack in the gel phase so as to *maximize the van der Waals interactions between the sn-1 chains*. In as much as the reported data show changes primarily in the thermal behavior of the saturated *sn*-1 chain, the large increase of approximately 20 °C in the T_m of PDPC compared to PAPC indicates that the saturated *sn*-1 chains in PDPC achieve a more stable packing environment relative to those of PAPC, whose *sn*-2 chain contains two less double bonds. The concomitant decrease in phase transition cooperativity from PAPC to PDPC suggests that the saturated *sn*-1 chains of PDPC also pack in smaller domains compared to those of PAPC.

Direct comparisons of changes in relative inter- and intramolecular order as a function of unsaturation are difficult since the order parameters derived for the *sn*-1 chains of PAPC and PDPC are dependent upon the integrity of the spectral subtractions of the analogous acids. Although this subtraction does not affect a determination of the phase transition temperatures or observed phase transition cooperativities, spectral subtraction can alter the order parameters derived from the Raman peak height intensity ratios. However, by performing numerous subtractions under different conditions, we estimate that the ordinate values shown in Figure 3 contain a maximum of a 5–10% error. Despite this uncertainty, the data still show, for example, that the gel-phase intensity parameters exhibit an increase in order for PAPC (Figure 3B,E) relative to POPC (Figure 3C,F). The increase in the I_{2935}/I_{2880} parameter, which contains an intrachain contribution, is likely a direct result of imposed order on the saturated *sn*-1 chain by the unsaturated *sn*-2 chain. Evidence for POPC exists indicating that the saturated chain methylene groups adjacent to the double bond in POPC show increased order relative to the remainder of the saturated chain (Seelig & Seelig, 1977). However, it is likely that the increased density of double bonds in PAPC relative to POPC gives rise to increased gel-phase lattice defects which are expressed as a reduction in phase transition or chain melting temperature. The observed increase, however, in the I_{2935}/I_{2880} indices containing intramolecular disorder of PDPC relative to PAPC (Figure 3C) implies that the increase from four to six double bonds in the *sn*-2 chain leads to a decrease in the average *sn*-1 chain order. That is, an increased PAPC gel-phase order arises from the van der Waals interactions between the additional methylene groups occurring near the bilayer center as a consequence of the two fewer double bond moieties.

The decreased cooperativity of the PDPC phase transition region indicates the existence of smaller lipid domains for the melting process relative to that of PAPC. While the higher T_m for PDPC suggests more stable domains for this lipid species, the I_{2935}/I_{2880} parameters increase toward greater disorder for PDPC bilayers. This increase in overall lipid intramolecular disorder in going from PAPC to PDPC (Figure 3E,F shows that the purely intermolecular disorder indices remain unchanged between PAPC and PDPC) occurs because the aggregates of smaller lipid domains of PDPC result in increased populations of disordered lipids at the domain interfaces (Devlin & Levin, 1989). Thus, these disordered interfacial lipids become a greater fraction of the total lipid ensemble. The nonlinearity in the observed I_{2935}/I_{2880} order/disorder parameters with increasing unsaturation is therefore consistent with the changes in the observed phase transition temperatures. Studies are presently being carried out with lipids containing perdeuterated *sn*-2 chains in order to obviate the need for spectral subtractions and to readily provide a convenient means for directly comparing the relative gel and liquid-crystalline order of these three lipid species.

Recent fluorescence depolarization measurements have characterized a bulk lipid bilayer parameter, the fractional volume (f_v), which is related to the acyl chain packing free volume (Straume & Litman, 1988). This parameter was, for example, linearly correlated with the equilibrium constant for the conformational interconversion of metarhodopsin I to metarhodopsin II (Mitchell et al., 1990). These studies showed that the conformational equilibrium of an integral membrane protein can be modulated by a global bilayer physical property whose value can be systematically changed by varying either the lipid *sn*-2 acyl chain unsaturation, the bilayer temperature, or the bilayer cholesterol content. The current vibrational Raman studies may provide an explanation of how an increase in the acyl chain packing free volume, as characterized by f_v, can facilitate a protein conformational change. If the microdomain character of the gel-phase and phase transition regions of PAPC and PDPC persists into the liquid-crystalline phases, then the packing efficiency of the acyl chains of these systems decreases relative to that of bilayers containing more saturated acyl chains. A positive bilayer volume change, such as that associated with the metarhodopsin I to metarhodopsin II interconversion, could be better accommodated in the polyunsaturated systems than in the more saturated chain bilayers if a coalescence of several microdomains into a larger domain resulted in an increase in acyl chain free volume within the hydrophobic region of the bilayer. This event would, in turn, allow the protein to undergo its conformational change. The regulation of acyl chain unsaturation, and hence the degree of microdomain heterogeneity, may provide a mechanism by which organisms can control bilayer physical properties responsible for optimizing various membrane functions associated with integral proteins.

References

Devlin, M. T., & Levin, I. W. (1989) *Biochemistry 28*, 8912–8920.

Gaber, B. P., & Peticolas, W. L. (1977) *Biochim. Biophys. Acta 465*, 260–274.

Huang, C., Lapides, J. R., & Levin, I. W. (1982) *J. Am. Chem. Soc. 104*, 5926–5930.

Keough, K. M. W., Giffin, B., & Kariel, N. (1987) *Biochim. Biophys. Acta 902*, 1–10.

Kouaouci, R., Silvius, J. R., Graham, I., & Pezolet, M. (1985) *Biochemistry 24*, 7132–7140.

Lavialle, F., & Levin, I. W. (1980) *Biochemistry 26*, 6044–6050.

Levin, I. W. (1984) *Adv. Raman Spectrosc. 11*, 1–49.

Lewis, E. N., Bittman, R., & Levin, I. W. (1986) *Biochim. Biophys. Acta 861*, 44-52.
McMurchie, E. J. (1988) in *Advances in Membrane Fluidity, Vol. 3, Physiological Regulation of Membrane Fluidity* (Aloia, R. C., Curtain, C. C., & Gordon, L. M., Eds.) pp 189-237, Alan, R. Liss, New York.
Mendelsohn, R., & Koch, C. C. (1980) *Biochim. Biophys. Acta 598*, 260-271.
Miljanich, G. P., Sklar, L. A., White, D. L., & Dratz, E. A. (1979) *Biochim. Biophys. Acta 552*, 294-306.
Mitchell, D. C., Straume, M., Miller, J. L., & Litman, B. J. (1990) *Biochemistry 29*, 9143-9149.
Mushayakarara, E., Albon, N., & Levin, I. W. (1982) *Biochim. Biophys. Acta 686*, 153-159.
Nielsen, N. C., Fleischer, S., & McConnell, D. G. (1970) *Biochim. Biophys. Acta 211*, 10-19.
Poincelot, R. P., & Abrahamson, E. W. (1970) *Biochemistry 9*, 1820-1825.
Seelig, A., & Seelig, J. (1977) *Biochemistry 16*, 47-50.
Snyder, R. G., & Schachtschneider, J. B. (1963) *Spectrochim. Acta 19*, 85-116.
Snyder, R. G., & Scherer, J. R. (1979) *J. Chem. Phys. 71*, 3221-3228.
Snyder, R. G., & Strauss, H. L. (1982) *J. Phys. Chem. 86*, 5145-5150.
Snyder, R. G., Hsu, S. L., & Krimm, S. (1978) *Spectrochim. Acta 34A*, 395-406.
Straume, M., & Litman, B. J. (1987) *Biochemistry 26*, 5113-5120.
Straume, M., & Litman, B. J. (1988) *Biochemistry 27*, 7723-7733.
Thompson, T. E., & Huang, C. (1986) in *Physiology of Membrane Disorder*, 2nd ed. (Andrioli, T. E., Hoffman, J. F., Fanestil, D. D., & Schultz, S. G., Eds.) pp 25-44, Plenum, New York.
White, D. A. (1973) in *Phospholipid Composition of Mammalian Tissues* (Ansell, G. B., Hawthorne, J. N., & Dawson, R. M. C., Eds.) p 441, Elsevier Scientific, New York.

Assembly of a Class I tRNA Synthetase from Products of an Artificially Split Gene†

Jonathan J. Burbaum and Paul Schimmel*
Department of Biology, Massachusetts Institute of Technology, Cambridge, Massachusetts 02139
Received October 29, 1990; Revised Manuscript Received November 21, 1990

ABSTRACT: The aminoacyl-tRNA synthetases arose early in evolution and established the rules of the genetic code through their specific interactions with amino acids and RNA molecules. About half of these tRNA charging enzymes are class I synthetases, which contain similar N-terminal nucleotide-fold-like structures that are joined to variable domains implicated in specific protein–tRNA contacts. Here, we show that a bacterial synthetase gene can be split into two nonoverlapping segments. We split the gene for *Escherichia coli* methionyl-tRNA synthetase (a class I synthetase) at several sites near the interdomain junction, such that one segment codes for the nucleotide-fold-containing domain and the other provides determinants for tRNA recognition. When the segments are folded together, they can recognize and charge tRNA, both in vivo and in vitro. We postulate that an early step in the assembly of systems to attach amino acids to specific RNA molecules may have involved specific interactions between discrete proteins that is reflected in the interdomain contacts of modern synthetases.

Because of their role in interpreting the genetic code, the aminoacyl-tRNA synthetases were among the earliest proteins (Rich, 1962; Woese, 1970). The three-dimensional structures of three class I enzymes, the tyrosyl- (from *Bacillus stearothermophilus*; Bhat et al., 1982; Blow & Brick, 1985), methionyl- (from *Escherichia coli*; Brunie et al., 1990), and glutaminyl-tRNA synthetases (from *E. coli*; Rould et al., 1989), show that these enzymes adopt similar N-terminal nucleotide-fold motifs, even though their primary sequences show only limited similarity (Schimmel & Söll, 1979; Schimmel, 1987). Structural modeling and sequence comparisons suggest a similar N-terminal nucleotide fold for the remaining class I synthetases (Burbaum et al., 1990). [In contrast, the class II synthetases contain no nucleotide binding fold (Eriani et al., 1990; Cusack et al., 1990).] In the class I synthetases, the site of amino acid binding and activation is found within the nucleotide binding fold (Brick & Blow, 1987), and as shown in the cocrystal of $tRNA^{Gln}$ with the glutaminyl-tRNA synthetase (Rould et al., 1989), the 3′-end of the tRNA substrate can be docked near the active site through interactions with a structural element that is inserted into this fold. In contrast, interactions with other portions of bound tRNA are facilitated through separate domains that are structurally unrelated to one another.

E. coli methionyl-tRNA synthetase is an α_2 dimer containing identical polypeptides of 676 amino acids (Dardel et al., 1984). Limited proteolysis generates an active monomeric fragment of about 550 amino acids (Cassio & Waller, 1971), whose crystal structure has been reported (Brunie et al., 1990). The N-terminal domain (360 amino acids) of the monomer is organized as a nucleotide fold with alternating α-helices and β-strands, while the C-terminal domain ($\sim$190 amino acids)

† This work was supported by NIH Grant GM23562 and a grant from the New Energy Development Organization of the Ministry of International Trade and Industry of Japan. J.J.B. is an NIH postdoctoral fellow, Grant GM12122.
* To whom correspondence should be addressed.

0006-2960/91/0430-319$02.50/0